

## Electrochemical Investigations on Liquid-State Polymerizing Systems: Case of Sol–Gel Polymerization of Transition Metal Alkoxides

Hélène Cattey,<sup>†</sup> Pierre Audebert,<sup>\*,‡</sup> Clément Sanchez,<sup>‡</sup> and Philippe Hapiot<sup>§</sup>

*Laboratoire de Chimie et Electrochimie Moléculaire, Université de Franche Comté, La Bouloie, Route de Gray, 25030, Besançon, Cedex, France, Laboratoire de Chimie de la Matière Condensée, URA CNRS no. 1466, Université de Paris 6, Place Jussieu, 75005, Paris, Laboratoire d'Electrochimie Moléculaire, URA CNRS no. 438, Université de Paris 7, 2 Place Jussieu, 75005, Paris, France*

*Received: May 7, 1997; In Final Form: October 20, 1997*

The polymerization kinetics of zirconium propoxide (and in a few cases of titanium butoxide) were studied in various conditions by following the diffusion of an electroactive probe attached to the metal center. Two different probes were considered, implying the complexation of the metal alkoxides with bidentate ligands functionalized by ferrocene moieties, respectively, a substituted acetylacetone (acac) ligand, and a stronger complexing ligand as a salicylate ligand. The polymerization kinetics can be followed with good accuracy on a real time scale by investigating the variation of the diffusion coefficients of the bounded ferrocenes. This variation can be related to the mass increase of the oligomers formed during the hydrolysis/condensation process. Electrochemical probing with the functionalized acac ligand shows that some decomplexation of the ligand occurs during the polymerization process. On the contrary, the salicylate ligand was irreversibly linked to the metal centers for the alkoxide precursor and also for the larger formed oxopolymers, allowing an accurate measurement of the mass variation of the electroactive species. The electrochemical results have been compared with information provided by other techniques. The influence of the electron self-exchange reaction between species with different diffusion coefficients on the measured diffusion coefficient was considered in the global analysis.

### Introduction

The sol–gel chemistry of silicon alkoxides, and more recently of transition metal alkoxides, is arousing more and more interest.<sup>1</sup> In addition to numerous spectroscopic investigations of sol–gel interactions with techniques such as nuclear magnetic resonance (NMR) spectroscopy,<sup>2</sup> we have recently developed an electrochemical approach to investigate the microviscosity changes of silica sols and gels. This method is based on the in situ determination of diffusion coefficients of an included electroactive species, that can be embedded<sup>3</sup> or bounded<sup>3b,c</sup> to the silicon species. A further development of this method is to irreversibly link the electroactive probes to the soluble polymerizing species and to investigate the changes in the diffusion rate of these growing oligomers at different stages of the polymerization process. In this case, the diffusion coefficient would correspond to the diffusion of the growing oligomer, which allows us to investigate changes of their sizes. This approach has the advantage of allowing the investigation of fast changes in the sol–gel structure during the polymerization process, which is much more difficult to achieve by a technique like NMR.

In the case of transition metal sol–gel, the alkoxide precursors are very reactive, and complexation of the metal is frequently used to reduce this reactivity to get sols and/or gels and to avoid the formation of precipitates.<sup>4</sup> Exchange of one alkoxy group by a bidentate ligand like acetylacetone increases the coordination number of the metal and decreases enough the reactivity

of a given alkoxide to enable the control of the polycondensation process through a sol–gel route.<sup>4a,b</sup> The alkoxy groups are always hydrolyzed prior to the chelating ligand. The complexing power depends both on the nature of the ligand and of the metal, and it decreases in the orders  $\text{Zr} > \text{Ti} > \text{Sn}$ , and salicylate  $>$  acac  $>$  carboxylic acid.<sup>1</sup> Zirconium is well adapted to our studies, because a salicylate-chelating ligand is totally resistant to the hydrolysis, even in pure water.<sup>5</sup> Thus, using this ligand, it is possible to irreversibly bind the electroactive moieties to zirconium alkoxides and to the condensed species produced during the hydrolysis/condensation process. On the contrary, in the case of a weaker complexing ligand, an equilibrium may exist in solution between the free and the bound form of the complexant.<sup>6</sup>

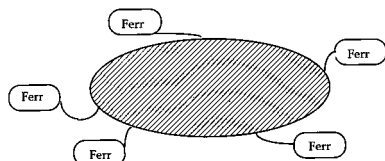
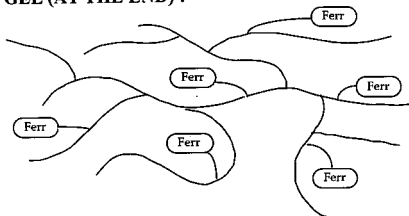
In this study, we have investigated the behavior of zirconium-based sol–gel systems with complexants, to which a small amount of the similar complexant that has been functionalized by a ferrocene has been added. This amount was sufficiently small to not modify the properties of the system, but can be used as an electrochemical probe to follow the change in the size of the oligomeric species. Diffusion kinetics of the attached ferrocene (i.e., of the oligomer) can be followed by transient electrochemical techniques (as chronoamperometry), and the diffusion coefficient can be measured from the current. From these values, information concerning the average size of the polymers or aggregates to which the functionalized complexant has bound itself, can be extracted. Scheme 1 illustrates this basal work hypothesis. However, during the polymerization process, oligomers with different sizes will be produced. It is well known that in similar situations the total current is not equal to the sum of each individual current because of the

<sup>†</sup> Laboratoire de Chimie et Electrochimie Moléculaire.

<sup>‡</sup> Laboratoire de Chimie de la Matière Condensée.

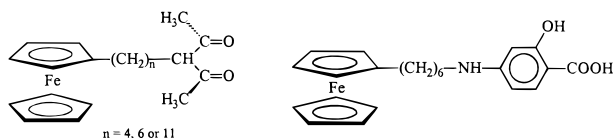
<sup>§</sup> Laboratoire d'Electrochimie Moléculaire.

\* Corresponding author.

**SCHEME 1: Diagram Symbolizing the Polymerization via the Sol–Gel Process, with Functionalized Monomers<sup>a</sup>****INITIAL STATE :****Monomers** $D = D_{\text{monomers}}$ **DURING THE POLYMERIZATION :****Oligomers** $D$  decrease**GEL (AT THE END) :****Polymers** $D = 0$ <sup>a</sup> The ferrocene species bind progressively to higher oligomers.

possible electron transfers between small and big oligomers. This problem has been addressed by single-step chronoamperometry in the case of a mixture of two molecules.<sup>7</sup> In our study, we have extended these calculations to the case of  $n$  species with fast isotopic electron exchange, and especially to the most encountered case of a Gaussian distribution of diffusing species. The relation between the average diffusion coefficient and the diffusion coefficient of the averaged mass species can be estimated from this model.

We have prepared the following functionalized complexants, where each of the complexing moieties are covalently bonded to a ferrocene species, with  $n$  taking selected values between 4 and 11:



We have used these electrochemical probes to investigate the polymerization of zirconium propoxide in the presence of either acetylacetone or ethylacetoacetate as the main complexant, with various hydrolysis and complexation ratios. The behavior of sols and gels based on the hydrolysis/condensation of titanium butoxide was also explored to a much smaller extent.

**Experimental Section**

**Synthesis of the Ligands.** The synthesis of two ligands, respectively, of the 3-[6-(1-ferrocenyl)hexyl]-pentanedione (Fc-acac) and 4-[6-amino(1-ferrocenyl)hexyl]salicylic acid (Fc-sal) type, stems from the same precursor with a six-methylene unit chain [1-(6-bromohexyl)ferrocene], which is produced in two

steps from ferrocene according to the following sequence. The synthesis of the other ligands, where the length of the chain varies (Fc-acac:  $n = 4, 6$ , and  $11$ ), occurs identically and has been omitted. All structures were confirmed by <sup>13</sup>C NMR and mass spectroscopy.

**1-(6-Bromohexanoyl)ferrocene.** First, 8.72 g ( $6.54 \times 10^{-2}$  mol) of AlCl<sub>3</sub> was added at 5 °C under N<sub>2</sub> to 13.37 g ( $7.19 \times 10^{-2}$  mol) of ferrocene dissolved in CH<sub>2</sub>Cl<sub>2</sub>. Then 10 mL ( $6.53 \times 10^{-2}$  mol) of 6-bromohexanoyl chloride dissolved in CH<sub>2</sub>Cl<sub>2</sub> was added in a dropwise manner to the preceding mixture. The solution was stirred for 10 min, and then returned to ambient temperature. The 1-(6-bromohexanoyl)ferrocene was obtained after hydrolysis on an ice/water mixture, an extraction with CH<sub>2</sub>Cl<sub>2</sub>, and chromatography (pentane 50%/diethyl oxide 50%). An orange oil was obtained: yield, 61%;  $F = 33$  °C; <sup>1</sup>H NMR: 4–5.5 ppm, m, 9H (ferrocenic protons); 3.4 ppm, t, 2H (–CH<sub>2</sub>Br–); 2.75 ppm, t (–CH<sub>2</sub>–CO–); 1.90 ppm, q (–CH<sub>2</sub>–CH<sub>2</sub>–Br); 1.70 ppm, q (–CH<sub>2</sub>–CH<sub>2</sub>–CO–); 1.50 ppm, q (central –CH<sub>2</sub>–).

**1-(6-Bromohexyl)ferrocene.** A standard Clemmensen reduction procedure was followed. First, 6.10 g ( $2.25 \times 10^{-2}$  mol) of HgCl<sub>2</sub>, 50 mL of distilled water, and 8 mL of concentrated HCl were added before introducing 79.15 g (1.21 mol) of activated zinc powder. The solution was stirred for 5 min and decanted. A mixture of 25 mL of water, 30 mL of concentrated HCl, and 60 mL of cyclohexane was added to the first solution with strong stirring. Then, 14.59 g ( $4.02 \times 10^{-2}$  mol) of 1-(6-bromohexanoyl)ferrocene was added. The mixture was heated at 100 °C for 6 h. Care should be taken to maintain a strong agitation or extensive deacylation may occur as a side reaction. The 1-(6-bromohexyl)ferrocene, again as an orange oil, was obtained after extraction with CH<sub>2</sub>Cl<sub>2</sub> and flash chromatography (pure pentane): yield (after chromatography), 64%;  $F = 33$  °C, <sup>1</sup>H NMR: 4 ppm, m, 9H (ferrocenic protons); 3.4 ppm, t, 2H (–CH<sub>2</sub>Br–); 2.35 ppm, t (–CH<sub>2</sub>–Fc); 1.90 ppm, q (–CH<sub>2</sub>–CH<sub>2</sub>–Br); 1.30–1.60 ppm, m, 6H (central –CH<sub>2</sub>s).

**4-[6-Amino(1-ferrocenyl)hexyl]salicylic acid (Fc-sal).** First, 0.41 g ( $2.68 \times 10^{-3}$  mol) of salicylic acid was dissolved in 3 mL of dry acetonitrile (3 Å molecular sieves), and 0.82 g ( $6.77 \times 10^{-3}$  mol) of 2, 4, 6-collidine and 0.85 g ( $2.43 \times 10^{-3}$  mol) of 1-(6-bromohexyl)ferrocene were added (addition of a few tenths of a milligram of oven-dried magnesium sulfate may be required). The mixture was heated for 6 to 8 days with stirring at 55 °C. The solution was extracted by diethyl oxide and washed several times with acidic water. The product was separated by flash chromatography (first 100% pentane, then dichloromethane was progressively added up to a 100% proportion). An orange solid was obtained: yield, 11%; <sup>1</sup>H NMR: 11.05 ppm, s, 1H, –NH–; 6–7.65 ppm, 3H, benzenic ring; 4.25, t, 2H (–CH<sub>2</sub>–NH–); 4.1 ppm, m, 9H (ferrocenic protons); 2.25 ppm, t (–CH<sub>2</sub>–Fc); 1.75 ppm, q (–CH<sub>2</sub>–CH<sub>2</sub>–NH–); 1.30–1.60 ppm, m, 6H (central –CH<sub>2</sub>s).

**3-[6-(1-Ferrocenyl)hexyl]pentanedione (Fc-acac).** In 5 mL of DMSO were added 2.87 g ( $2.87 \times 10^{-2}$  mol) of acetylacetone and 1.55 g ( $2.87 \times 10^{-3}$  mol) of sodium methylate. Then 5 g ( $1.43 \times 10^{-2}$  mol) of 1-(6-bromohexyl)ferrocene was added and the mixture was heated at 90 °C for 3 h. The product was neutralized with acidic water, then extracted with diethyl oxide and purified by flash chromatography (pentane 70%, diethyl oxide 30%): yield, 20%; <sup>1</sup>H NMR: 16.7 ppm, s, 1H, –O–H, enol; 4.1 ppm, m, 9H (ferrocenic protons); 3.6 ppm, t, 1H (CH–CO–)<sub>2</sub>; 2.4 ppm, t, 2H (CH<sub>2</sub>–CH=); 2.3 ppm, t, 2H (–CH<sub>2</sub>–Fc); 2.15 ppm, s, 3H (CH<sub>3</sub>–C=O); 2.1 ppm, s, 3H (CH<sub>3</sub>–C(OH)); 1.1–1.4 ppm, m, (central –CH<sub>2</sub>s).

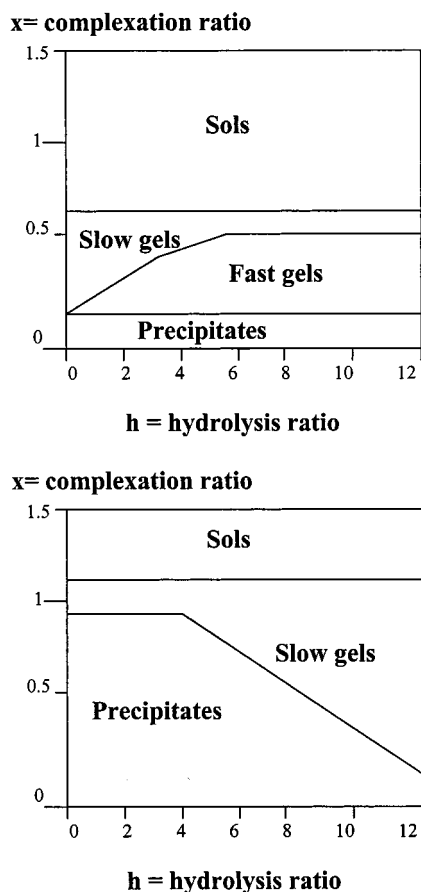


**Figure 1.** Gelification diagrams of  $\text{Zr(OPr)}_4$  for different complexants: upper, acetylacetone (acac); lower, ethyl acetoacetate (etacac).

**Gels Preparation.** Inside a tube-shaped thermostated cell were mixed  $\text{Zr(OPr)}_4$  (or in a few experiments,  $\text{Ti(O}^n\text{Bu)}_4$ ; for a typical experiment, 5 mL of a 70%  $\text{Zr(OPr)}_4$ /30% 2-propanol solution, a chosen  $x$  equivalent of complexant (acac or etacac,  $x$  being called complexation ratio in the following, expressed as [number moles of complexant]/[number moles of  $\text{Zr(OPr)}_4$ ]), a polar enough cosolvent made of 50% acetonitrile and 50% methanol (typically 15 mL), and 0.2 g of lithium perchlorate. Then,  $10^{-3}$  M of the functionalized complexant (Fc-acac or Fc-sal) was added, and cyclic voltammetry and chronoamperometry were performed. Then, a given amount of a 10% water/90% propanol hydrolysis solution was added with stirring (the amount of water is defined by the hydrolysis ratio  $h$  = [number moles of water]/[number moles of  $\text{Zr(OPr)}_4$ ]; because  $h$  was allowed to vary, the volume of the solution varied in accordance, and concentration corrections were made, consequently, in the diffusion coefficient determinations. For experiments carried out with titanium butoxide, only acac could be used as the main complexant. The hydrolysis ratios were carefully chosen to avoid precipitates. The gelification diagram (Figure 1) of the  $\text{Zr(OPr)}_4/\text{acac}$  and  $\text{Zr(OPr)}_4/\text{etacac}$  systems were determined separately from similar experiments, quoting the gelation times and nature (sols, clear gels, turbid gels or precipitates), but without the electroactive probe added. Gels were designated as "slow" when the gelation time was  $>1$  h, otherwise they were called "fast" gels. Usually, slow gelling times lead to transparent gels, whereas fast gelling times lead to opalescent or turbid gels. In the case of  $\text{Ti(O}^n\text{Bu)}_4/\text{acac}$ , the choice of  $h$  covered too narrow a range once  $x$  was fixed and the results (gels, sols) are directly quoted in the tables gathering the results. In addition, in a few cases, we checked and found that the small

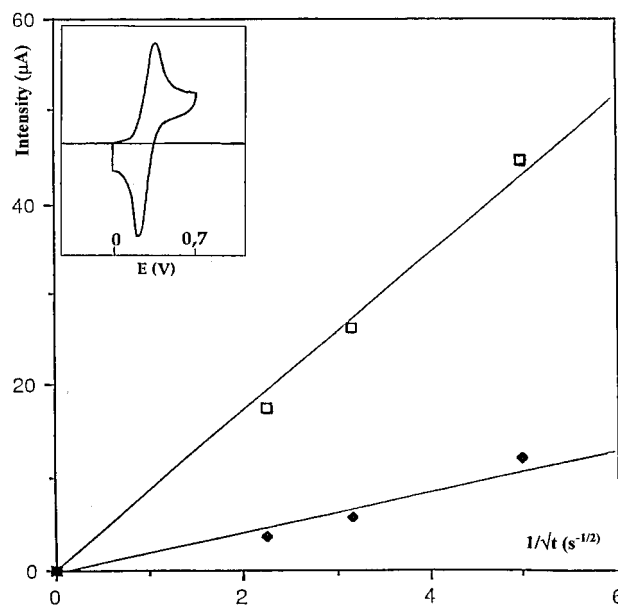


**Figure 2.** Cottrell plots obtained by chronoamperometry in the case of the system with Fc-sal/etacac at a complexation rate equal to 0.37 and a hydrolysis rate equal to 2. Features represents the evolution of the diffusion coefficient at the beginning of the polymerization reaction ( $\square$ ) and at the end of the polymerization ( $\blacklozenge$ ). The insert shows the voltamogram of the corresponding system obtained at 1V/s.

amount of electroactive probe did not affect the gelification process at all, as expected.

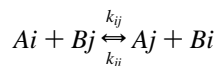
**Electrochemical Measurements.** After a first experiment to check the monomer behavior, the electrochemical study was started as soon as the addition of water has ended ( $\sim 20$  s). For main course studies, the electrochemical setup consisted of a 1.2-mm diameter glassy carbon electrode, a platinum counter electrode, and a calomel electrode connected to a homemade potentiostat<sup>8</sup> equipped with an ohmic drop compensation device. The chronoamperometry experiments were performed stepping from 0 to +0.7 V (which is  $>200$  mV beyond the ferrocenes potential peaks in the sols). The data were collected on a Nicolet 350 digital oscilloscope, the whole experiment duration (data acquisition) being usually 1 or 2 s. A typical chronoamperometric curve is represented in Figure 2, and attests both the linearity of the Cottrell curve during the chosen time scale.

Several experiments were conducted in parallel using ultramicroelectrodes instead of conventional microelectrodes. In this case, the electrodes were 10- or 20-mm diameter gold. The data after digitalization were transferred to a PC computer for treatment. The diffusion coefficients were extracted using the equation devised by Shoup and Szabo<sup>9</sup> in conditions closed to the stationary currents (typical experiments were run for times between 0.5 and 10 s). In such conditions, the current could be approximate by  $i = (8/\pi^2) FSD^{1/2}C/(\pi r)^{1/2} + 4FDCr$  ( $S$ , surface area;  $D$ , diffusion coefficient;  $r$ , electrode radius). A plot of  $i$  as a function of  $t^{-1/2}$  (measuring the slope and the intercept, see the Supporting Information section for an example of such plot) allows an absolute determination of  $D$  and  $C$  if the radius of the electrode has been measured before. (With an ultramicroelectrode, the real radius of the electrode can be slightly different from the radius of the wire depending on the making of the electrode and the polishing.) In our experiments, only the relative variations of  $D$  and  $C$  were considered, but if we take the radius of the gold wire as the geometric radius of the electrode and suppose a perfect disk shape to estimate the surface, we found values of  $D$  in the  $10^{-5}$ – $10^{-6}$   $\text{cm}^2 \text{s}^{-1}$  range.

**Miscellaneous.** Calculations were performed on a PC computer with the help of a Matlab software. BET experiments were performed on dry xerogels on a Micromeritics 2100 A rapid surface area analyzer using N<sub>2</sub> as the adsorbed gas. Elemental analysis were performed on several xerogels after stabilization of the system and drying in air.

## Results

**Theoretical Background.** During the polymerization process, oligomers with different sizes are produced and the solution contains a distribution of electroactive species with different diffusion coefficients. Thus, we need to estimate the relation between the diffusion coefficients of such distribution and the electrochemical current recovered from chronoamperometry experiments. In this connection, we need to answer two main questions. First, how close is the current recovered to the sum of the currents arising from the contributions of the different electroactive species with different masses and diffusion coefficients? Second, extracting an average diffusion coefficient supposes that we are dealing with a centered distribution, which is the most often encountered case. Therefore, the related question is: How close is the central diffusion coefficient to the average measured diffusion coefficient (i.e., extracting the  $D$  value as if a single diffusing species were present in the solution) in case of a given definite distribution (e.g., a Gaussian distribution). The first question raises the problem that the total current is not equal to the sum of the individual currents for each species when the solution contains a mixture of species with different diffusion coefficients due to electron exchange between small and large molecules.<sup>10</sup> The problem has been previously addressed in the context of a mixture of two different reactants (see for example refs 7 and 11), including the case of interest for us, the homogeneous isotopic exchange<sup>7</sup> (all the electroactive species have the same standard potentials  $E^\circ$ ). In case of a fast electron exchange versus diffusion, it has been shown that the contribution of smaller species is expected to increase the current values.<sup>7,11</sup> In this particular case, an analytical solution can be obtained in the context of chronoamperometry in the previously nonexamined case of  $n$  species with  $n$  different diffusion coefficients  $D_1, \dots, D_n$ . Let us call  $A_i$  the oxidized species, with a bulk concentration equal to  $A^\circ_i$ , which can be reduced in  $Bi$  at the electrode according to the reaction:  $A_i + e^- \rightleftharpoons Bi$  and also exchange an electron with any of the reduced species  $B_j$  according to:



The system of differential equations describing this system can be written as follows:

$$\frac{\partial A_i}{\partial t} = D_i \frac{\partial^2 A_i}{\partial x^2} - \sum_j k_{ij} A_i B_j + \sum_j k_{ji} A_j B_i$$

with  $K = k_{ij}/k_{ji} = 1$ , and with the following initial conditions:

$$t = 0, x \geq 0 \text{ and } x = \infty, t \geq 0: A_i = A^\circ_i \text{ and } B_i = 0$$

$$x = 0, t \geq 0, A_i = 0 \text{ and } \frac{\partial A_i}{\partial x} + \frac{\partial B_i}{\partial x} = 0$$

because we suppose that the potential is negative enough for the concentration of any oxidizable species to be zero at the electrode. It is easier to use a dimensionless formulation, defining the following dimensionless variables:  $a_i = A_i/A^\circ_1$ ,  $b_i$

$= B_i/A^\circ_1$ ,  $d_i = D_i/D_1$ ,  $\tau = t/\theta$  (where  $\theta$  represents the measurement time), and  $\lambda_{ij} = k_{ij}A^\circ_1\theta$ . The dimensionless form of the current  $\psi$  would be then  $\psi = i\theta^{1/2}/FSD_1^{1/2}A^\circ_1$ , the letters having their usual signification. We are searching  $\psi$  which is equal to  $\sum_i d_i (\partial a_i / \partial y)_0$ . From our hypothesis on isotopic fast exchange, it comes  $\lambda_{ij} = \lambda_{ji}$  and  $a_i b_j / a_j b_i = 1$ ; therefore the sum  $a_i + b_i$  is constant throughout the solution. In particular this is true for  $j = 1$ , which leads to  $a_i = (A^\circ_i/A^\circ_1)(1 - b_1) = (A^\circ_i/A^\circ_1) a_1$ . Let us call  $\gamma_i$  the ratio  $A^\circ_i/A^\circ_1$ , so it becomes  $a_i = \gamma_i a_1$ . On the other hand, the sum of the partial derivative equations leads to:

$$\frac{\partial(\sum_i a_i)}{\partial \tau} = \sum_i d_i \frac{\partial^2 a_i}{\partial y^2}$$

replacing the  $a_i$  by  $\gamma_i a_1$ , it becomes:

$$(\sum_i \gamma_i) \frac{\partial a_1}{\partial \tau} = (\sum_i d_i \gamma_i) \frac{\partial^2 a_1}{\partial y^2}$$

Thus, since  $a_i = \gamma_i a_1$ :

$$\left(\frac{\partial a_i}{\partial y}\right)_0 = \gamma_i \left(\sum_i \gamma_i / \sum_i d_i \gamma_i\right)^{1/2} (\pi \tau)^{-1/2} \quad (1)$$

and therefore:

$$\psi = [(\sum_i d_i \gamma_i)(\sum_i \gamma_i)]^{1/2} (\pi \tau)^{-1/2} \quad (2)$$

Then,  $i$  becomes:

$$i = FS[(\sum_i D_i A_i)(\sum_i A_i)]^{1/2} (\pi \tau)^{-1/2} \quad (3)$$

This expression should be compared to the expression:

$$i = FS(\pi \tau)^{-1/2} \sum_i (D_i)^{1/2} A_i \quad (4)$$

which would be obtained without occurrence of the electron exchange.

Let us now turn toward the second problem of what would be the current  $i$  recovered from a Gaussian collection of species of mass  $m_i$  and concentrations  $C_i$  reduced at the same potential, with  $D_\mu$  being the diffusion coefficient of the most abundant species of mass  $\mu$  (midpoint of the Gaussian, concentration  $C_\mu$ ), with a given standard deviation  $\sigma$ , and with the sum of the concentrations equal to  $C^\circ$ . The expression (2) just derived is still valid. Let  $i_0 = FS C^\circ D_\mu^{1/2} (\pi \tau)^{-1/2}$  be the current recovered if all the species were  $\mu$  species, which is derived straightforwardly from a chronoamperometry experiment. We can normalize the currents relative to  $i_0$ :

$$i/i_0 = (1/C^\circ D_\mu^{1/2}) [(\sum_i D_i C_i)(\sum_i C_i)]^{1/2} = \left[ \left( \sum_i \left( \frac{D_i C_i}{D_\mu C^\circ} \right) \right) \left( \sum_i \frac{C_i}{C^\circ} \right) \right]^{1/2} \quad (5)$$

If we are in the presence of a Gaussian distribution, hence we have:

$$\frac{C_i}{C^\circ} = (1/\sqrt{2\pi}\sigma) \exp[-(m_i - \mu)^2/2\sigma^2] \mu$$

designing the average mass and  $\sigma$  the standard deviation. If the Stokes-Einstein law applies,

$$D_i/D_\mu = (m_i/\mu)^{1/3}$$

Therefore, shifting to the integral form of the equation, we have, in the case where diffusion-coupled electron exchange is considered:

$$i/i_0 = [1/(\sigma\sqrt{2\pi})][(\int_{m^\circ}^{\infty} (m/\mu)^{1/3} \times \exp[-(m - \mu)^2/2\sigma^2] dm)(\int_{m^\circ}^{\infty} \exp[-(m - \mu)^2/2\sigma^2] dm)]^{1/2} \quad (6)$$

where  $m^\circ$  represents the smallest mass present in the real distribution (monomer case if we consider a polymerizing system). The normalized current in the classical case is given by:

$$i/i_0 = [1/(\sigma\sqrt{2\pi})][\int_{m^\circ}^{\infty} (m/\mu)^{1/6} \exp[-(m - \mu)^2/2\sigma^2] dm] \quad (7)$$

In the case where the diffusion coefficient distribution is Gaussian (instead of the masses distribution as previously examined), it is easy to check that we can replace eqs 6 and 7 by eqs 6' and 7', where the  $(m/\mu)^{1/3}$  coefficient is replaced by simply  $m/\mu$ . The Figures 3 and 4 display calculated values according to  $m^\circ$ ,  $\mu$  chosen equal to 5  $m^\circ$  and  $\sigma$ . The value of  $m^\circ$  is arbitrarily chosen as 1. Curves 3a and 3b represent the normalized currents recovered from a collection of diffusing species with a Gaussian mass distribution, either in a classical approach (without coupled electron transfer) or with electron-transfer considered. It is clear that the curves display the same behavior, and we see that the currents closely reflect the average species current, until the standard deviation  $\sigma$  does not exceed 40% of the  $\mu$  value. Figure 3c gives the ratio between the two currents; that is, focuses on the possible influence of the electron transfer. It is clear that the effects are very weak, as would be expected, but the theoretical current in the presence of electron transfer gets slightly higher when a lot of small species are present. This result is in accordance with literature predictions in more simple cases,<sup>7</sup> because smaller species can diffuse faster and after exchange contribute more to the total current. Figure 4a, b, and c represent the three kinds of curves previously described. However, the case where the diffusion coefficients (and no longer the masses) of the species have a Gaussian distribution is the only case where the average diffusion coefficient is five-fold the monomer one. It can be seen that qualitatively identical effects are obtained, albeit with a noticeable enhancement because the dependence of the diffusion coefficient with the mass is the cubic root.

In conclusion, the average experimental diffusion coefficient that can be extracted from a chronoamperometry experiment performed on a Gaussian collection of species reflects with a reasonable accuracy the diffusion coefficient of the central species. More generally, even when the distribution is not Gaussian, it is likely that the average  $D$  value extracted from chronoamperometry experiments is close to the real average  $D$  values of the diffusing species.

**Polymerization of Zirconium Propoxide.** *Choice of the Ligand.* Bidentate ligands are commonly used to decrease the zirconium propoxide reactivity. Earlier works have shown that

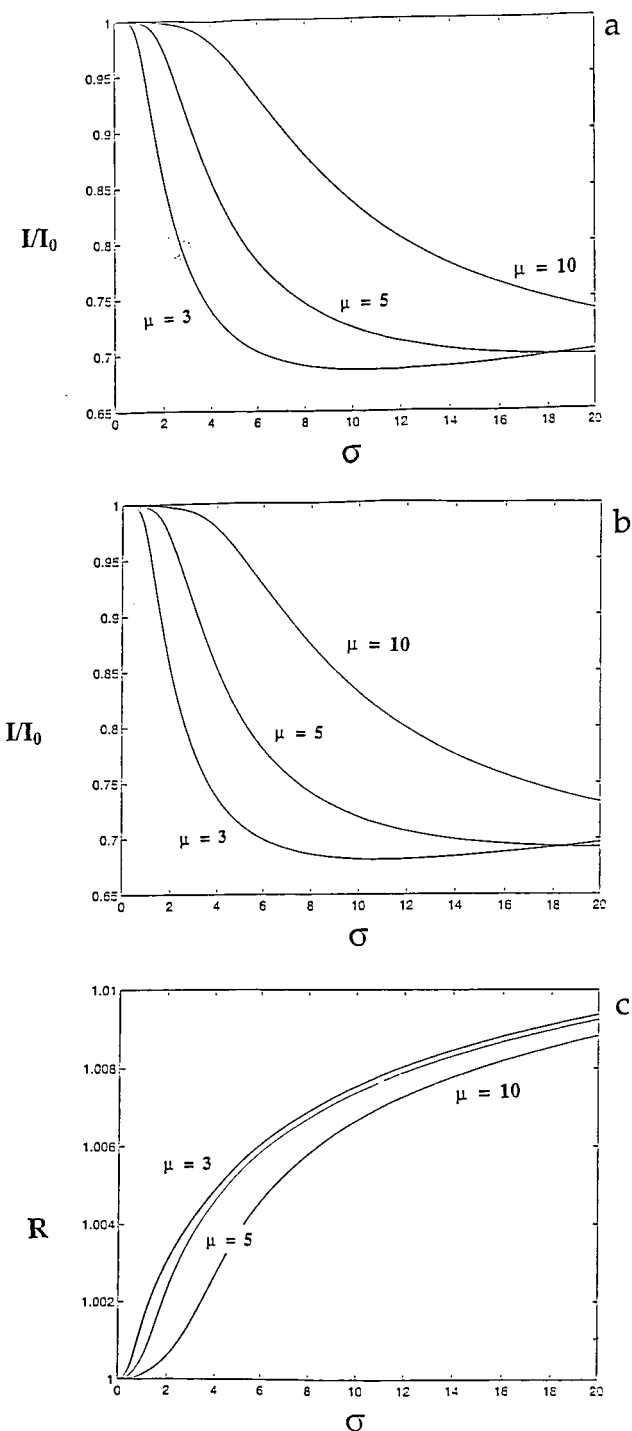


**Figure 3.** Theoretical variation of the normalized current ratio  $I/I_0$  in the (a) absence or in the (b) presence of diffusion-coupled electron exchange, for a collection of electroactive species with a Gaussian mass distribution, in function of the average mass  $\mu$  and the standard deviation  $\sigma$ . See text for  $I$  and  $I_0$  definition. The mass  $\mu$  is given in units of the lowest mass present (monomer case) for three selected cases of 3, 5, and 10. (c) Ratio of the two curves (a) and (b) [ $R = I$  (with electron exchange)/ $I$  (without electron exchange)].

ethyl acetoacetate (etacac),<sup>3c,12</sup> acetylacetone (acac)<sup>3c,13</sup> and salicylic acid (sal)<sup>5,6</sup> were efficient ligands, which substituted readily with the propylate moieties on the metal. Previous NMR and chemistry studies have shown that the complexation strength rises in the order etacac < acac < sal. Whereas etacac binds reversibly, acac binds irreversibly, but may be released by an excess of water. On the contrary, sal is not released, even in pure water, because it has been demonstrated that zirconium

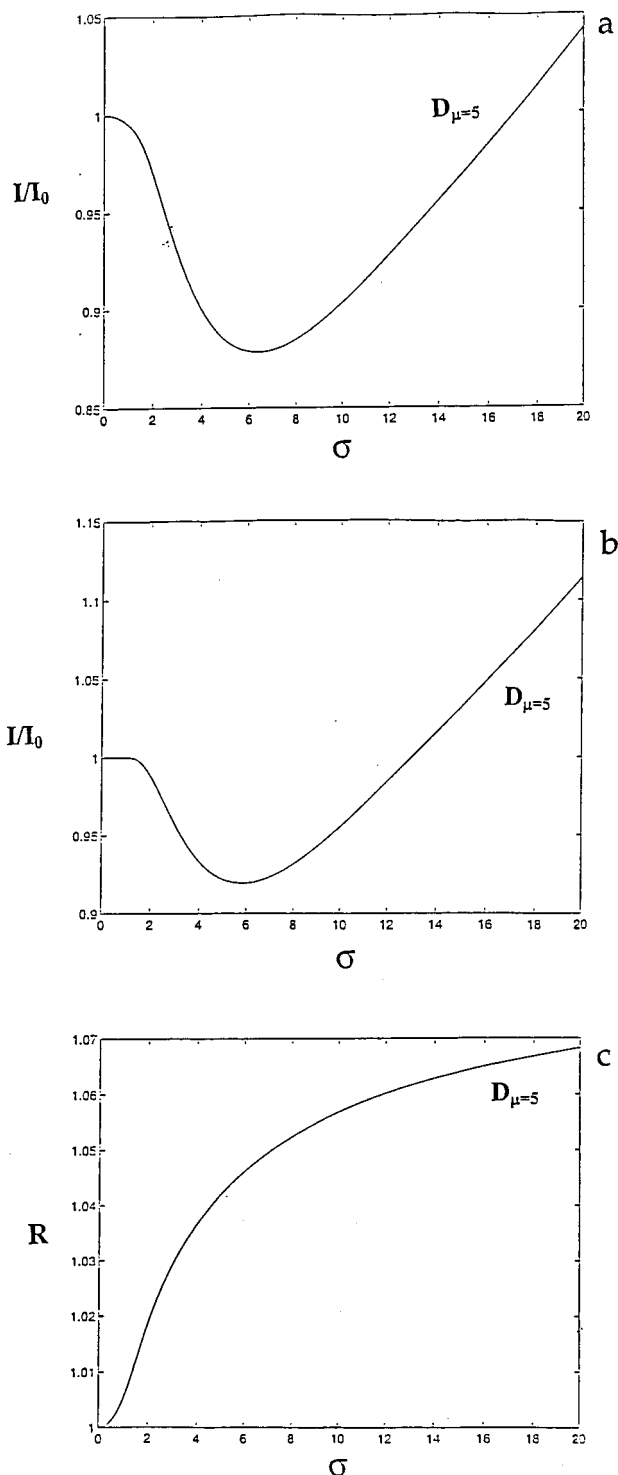


**Figure 4.** Same feature as in Figure 3 for a collection of species with a Gaussian distribution of diffusion coefficients centered on an average diffusion coefficient  $D_\mu$  which is equal to five times the one of the smallest species.

salicylate is stable, in pure water.<sup>5</sup> Our functionalized ligands can be expected to bind slightly less strongly than the parent unsubstituted ligand (i.e., when the part of the molecule binding to the metal has the same chemical structure) mainly because of steric effects. If we want that the functionalized ligands remain attached to the oligomers in formation, the main complexant of the system should be a weaker ligand than the functionalized one. It is also obvious that the functionalized ligand must not be removed upon hydrolysis. Two systems were studied  $\text{Zr}(\text{O}^n\text{Pr})_4/\text{etacac}$  and  $\text{Zr}(\text{O}^n\text{Pr})_4/\text{acac}$ . For each system,

two different probes were considered: Fc-acac and Fc-sal. When etacac is the main ligand, both Fc-acac and Fc-sal probes are expected not to be released from the zirconium polymers, as in the case of Fc-sal in the  $\text{Zr}(\text{O}^n\text{Pr})_4/\text{acac}$  system. Only in the last case,  $\text{Zr}(\text{O}^n\text{Pr})_4/\text{acac}$  with Fc-acac, the competition between the main acac ligand and the functionalized Fc-acac can be slightly unfavorable toward hydrolysis. However, in all cases, propylate is always hydrolyzed first, and the removal of the ligand from the growing species should not be felt at the early stage of the condensation. Besides, the difference between the electrochemistry of Fc-sal and Fc-acac labeled alkoxides when acac is the main ligand was expected to give valuable information on ligand release in the latter case.

**Gelification Diagrams.** Prior to the electrochemical study, it was necessary to determine the gelification diagram of the zirconium propoxide in the presence of the two complexing ligands that we used; namely, etacac (weak complexing ligand) and acac (strong complexing ligand). No reports were available in the former case. Even though some reports existed with acac, the use of slightly different solvents suitable for electrochemistry made the determination of the gelification parameters useful. The Figure 1 shows the results obtained in the case of the two systems studied; it is clear that both system behave as previously noticed in analogous cases, with precipitation of zirconium oxopolymers in all cases with a weak complexing ratio  $x$  and on the contrary, stable sols above a given  $x$  value. However, the intermediate gel zone shows a difference between the two systems. Although there is no detectable influence of the hydrolysis ratio  $h$  in the case of the relatively strong complexing ligand acac,  $h$  influences the gelification in the case of etacac, probably as a consequence of the easier hydrolysis of this weaker ligand.

**Electrochemical Results.** As expected, the chronoamperometry currents decrease upon sol aging and in the course of the gels formation. Several complexing ratios ( $x$ ) and hydrolysis ratios ( $h$ ) values were investigated, both in the sol and gel regions. The results of all electrochemical studies will be presented in terms of the mean diffusion coefficient variation extracted from the Cottrell current in potentiostatic conditions. As explained before, the experimental measured variation is  $C_{\text{ferrocene}} D^{1/2}$ . Assuming that the concentration of ferrocene (i.e., of the functionalized ligand) does not change during the polymerization process, the value of the variation of the diffusion coefficient can be extracted. Most of our experiments were performed in the sols or gels conditions, all absolute diffusion coefficients values were in the  $10^{-5}$ – $10^{-6}$   $\text{cm}^2 \text{s}^{-1}$  range using the geometric parameters of the electrode. Only in the very few cases where the precipitates were studied, we observed lower  $D$  values, which were not lower than  $10^{-7}$   $\text{cm}^2 \text{s}^{-1}$ . Therefore, physical diffusion is the main process in our systems, as would be expected from such highly solvated medium.<sup>3</sup> To check that the concentration of ferrocene does not change significantly during the polymerization, we performed the same set of experiments as previously detailed, using micron size ultramicroelectrodes instead of classical millimeter size microelectrodes. This method is based on the comparison between the planar diffusion current and the steady-state current on the same electrode and allows the determination with the same experiment of two parameters of the system.<sup>14</sup> This procedure has been used to determine  $D$  independently from the electrode area<sup>14</sup> or the number of electron exchange by molecule,<sup>14a</sup> but it is also possible to determine  $D$  independently from the concentration of the electroactive species if the radius of the electrode is known. We thus calculated the variation of the  $D$

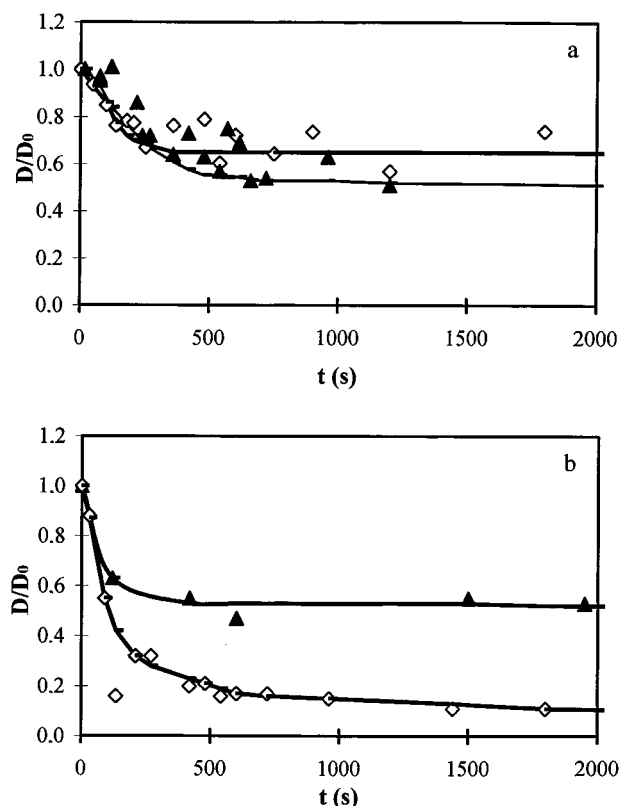


**Figure 5.** Variation of diffusion coefficients with time and influence of the probe: (a) etacac,  $x = 0.75$  and  $h = 10$ ; (b) acac,  $x = 0.4$  and  $h = 4$  with as ligands for the two curves, Fc-sal (◇) or Fc-acac (▲) as electroactive probe.

values independently from the concentrations of ferrocene as explained in the experimental section. It is difficult to get precise absolute values for the diffusion coefficient because of the uncertainties of the electrode radius<sup>14b</sup> and area then only the relative variations were considered. Similar variation of the extracted diffusion coefficient were observed, showing that reproducibility is encountered independently from the used technique (see Supporting Information section for a comparison of the variations of  $D$  by the two methods). In addition, this precaution ensures that we are indeed dealing with a diffusion coefficient decrease and not concentration depletion in the gels, thus corroborating our ground hypotheses.

**Influence of the Probe Nature.** To elucidate if probe release had to be taken into consideration and to that extent, we investigated the electrochemical response of two identical systems, on one hand with acac and on the other with etacac as the main complexant. In each case, either the Fc-acac probe or the Fc-sal probe was used. Figure 5 shows the response of identical systems (same complexing and hydrolysis ratio), with etacac or acac as the main complexing agent, and with either Fc-sal or Fc-acac as the electroactive probe. The curves displayed in Figure 5a show that, as expected, identical responses are obtained when etacac is the main ligand, whatever the probe complexing strength. Both the time dependence and the plateau of the  $D(t)$  curves are the same; the probe release is therefore negligible in the course of the experiment, and the  $D$  variation is related to the dynamics of the alkoxide hydrolysis in this case. On the contrary, when acac is the main ligand (Figure 5b), different curves are displayed for closely related systems, differing only by the probe nature. It is obvious this time that the  $D$  decrease is much smaller when Fc-acac is used as the probe, certainly as a consequence of the unfavorable competition between Fc-acac and acac complexation. The

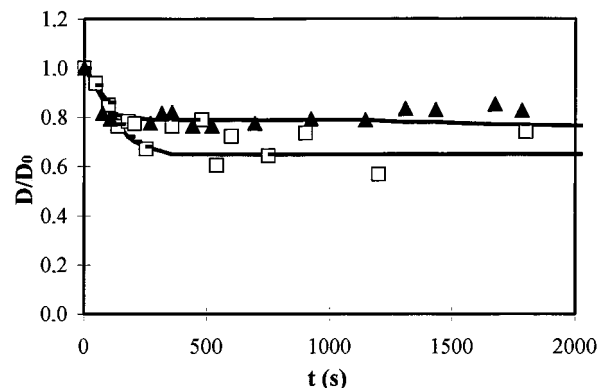


**Figure 6.** Variation of diffusion coefficients with time and influence of the main complexant. Fc-sal was always used as the probe with either acac (▲) or etacac (□) as main complexant.

relatively high  $D$  plateau probably reflects the existence of free Fc-acac released in the solution. On the other hand, the low  $D$  plateau when Fc-sal is the probe should be related to the existence of highly aggregated species in this case.

**Influence of the Complexation and Hydrolysis Ratio.** From the gelification diagrams, it is evident that the complexation ratio (proportion of the main complexant initially added to the system) is the most relevant parameter to predict the final state of the system. It is possible to correlate the  $D$  curves, and especially the  $D$  plateaus to the complexation ratio, either with acac or etacac as the main ligand. However, in the case of etacac, the gel domain is quite narrow. Thus, changing  $x$  values over a wide range results in the obtention of sols on one hand, and turbid gels or even precipitates on the other hand. Because Fc-sal was found to give the most reliable data in our systems without any release from the oxopolymers, whatever the main ligand nature, the use of this probe was chosen through the rest of this work.

**Influence of the Main Complexant Nature.** Figure 6 shows the compared behavior of two systems that differ only by the complexant kind: namely, acac or etacac. It is clear that although the kinetics appear similar, the  $D$  plateaus differ noticeably. The higher value obtained in the case of acac shows that, as expected with this stronger complexant, the average condensation degree is much lower, resulting in the formation of smaller oligomers. The opposite behavior is observed in the case of the weaker complexant etacac.

**Influence of  $x$  and  $h$ .** The curves in Figure 7 show that the  $D$  plateaus change very regularly according to the complexation ratios with etacac as the main complexant. As expected high complexation ratios lead to weakly condensed, fast diffusing species, whereas low complexation ratios lead to highly condensed aggregates and very low  $D$  values. The same behavior is again seen when acac is the main ligand, as shown in Figure 7b. Again, the  $D$  values vary strongly contrariwise to the complexation ratio. On the contrary, the hydrolysis ratio appears to have a weak influence on the  $D$  values, and correlatively also with the nature of the condensed species. This is obvious in the case of acac (as shown in Figure 8), but even in the case of etacac,  $D$  plateaus are found in the same range whatever the  $h$  value. However, we tried to generate oxopolymers and never tried very weak hydrolysis ratios ( $<2$ ), which should have lead to small molecular weight clusters.<sup>1b</sup>

**BET Measurements and Elemental Analysis.** Gas adsorption experiments allow the determination of specific surface area values of the dried xerogels. Of course the structure of the dried gel is different from the structure of the wet gel, but the size of

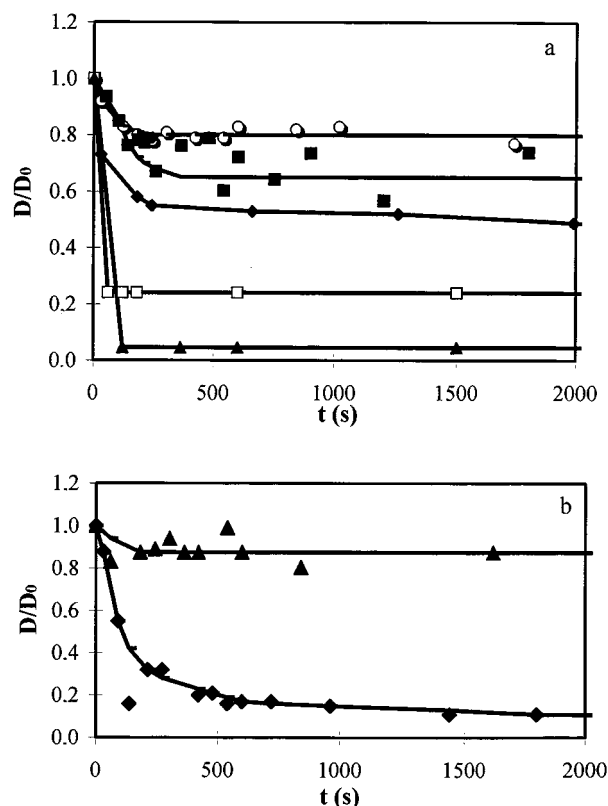


**Figure 7.** Variation of diffusion coefficients with time and influence of the complexation ratio. (a) The couple Fc-sal/etacac was studied throughout with several different  $x$ :  $x = 1.25$ ,  $h = 2$  (○);  $x = 0.75$ ,  $h = 10$  (■);  $x = 0.4$ ,  $h = 6$  (◆);  $x = 0.2$ ,  $h = 2$  (□);  $x = 0.1$ ,  $h = 2$  (▲); (b) The couple Fc-sal/acac was studied with two different  $x$ :  $x = 1.25$ ,  $h = 2$  (▲);  $x = 0.4$ ,  $h = 2$  (◆).

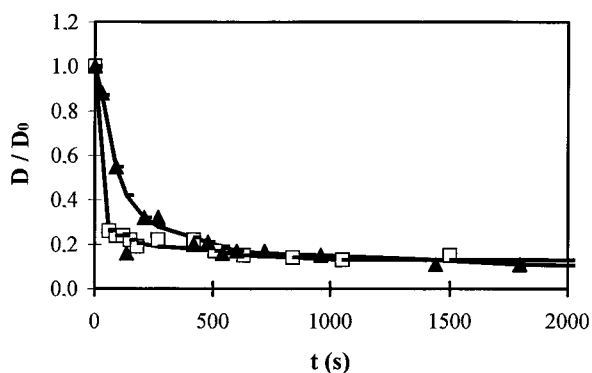


**Figure 8.** Variation of diffusion coefficients with time and influence of the hydrolysis ratio on the couple Fc-sal/acac. (a)  $x = 0.4$ ,  $h = 2$  (▲); (b)  $x = 0.4$ ,  $h = 6$  (□).

the pores has a relation with the average oxopolymer size in the fresh gel. Results in Table 1 show that the BET specific surface area values of the xerogels is in the 100 m<sup>2</sup>/g range. There is an increase with the hydrolysis ratio in the case of a good complexant like acac; on the other hand, the surface area is practically constant with the weak complexant etacac. The results of elemental analysis on carbon and hydrogen clearly show that all ligands remain inside the xerogels in the case of Fc-sal, and 90% to 100% in the case of Fc-acac, according to the case where the main ligand is etacac or acac, respectively. On the contrary, all propylate moieties are hydrolyzed and the propanol formed is then evaporated out of the final xerogel (because of the presence of little residual water, oxygen content does not provide reliable data). About the main ligand, analyses show the more labile etacac ligand is partly released, 60% to

**TABLE 1: Results Obtained by BET Measurements on Several Xerogels**

atom	complexant	complexation ratio	hydrolysis ratio	BET (m <sup>2</sup> /g)
Zr	Acac	0.45	4	130
	Acac	0.5	2	82
	Acac	0.5	4	140
Zr	Acac	0.5	10	231
	Etacac	0.6	10	73
	Etacac	0.7	10	105
Ti	Etacac	1	10	92
	Acac	0.5	15	221
Ti	Acac	0.3	18	44
	Etacac <sup>a</sup>	0.9	4	6

<sup>a</sup> Precipitate.

**TABLE 2:  $D$  Plateau Values Obtained from the Hydrolysis of Ti(O<sup>n</sup>Bu)<sub>4</sub> with the Fc-acac/acac Couple, In Function of the Complexation Ratio  $x$  and the Hydrolysis Ratio  $h$**

complexation ratio	hydrolysis ratio	Diffusion coefficient		Aspect
		initial	final	
0.30	18	1	1.00	slow gel (5 hours)
0.35	19	1	0.90	slow gel (2 days)
0.40	17	1	0.97	slow gel (2 days)
1.25	2	1	0.88	stable sol
1.25	4	1	1.00	stable sol

**TABLE 3:  $D$  Plateau Values Obtained from the Hydrolysis of Ti(O<sup>n</sup>Bu)<sub>4</sub> with the Fc-sal/acac Couple, In Function of the Complexation Ratio  $x$  and the Hydrolysis Ratio  $h$**

complexation ratio	hydrolysis ratio	diffusion coefficient		aspect
		initial	final	
0.30	19	1	0.26	slow gel (1.5 days)
0.35	13	1	0.53	slow gel (2.5 days)
0.40	16	1	0.22	slow gel (3 days)
1.00	2	1	0.94	stable sol
1.25	2	1	1.00	stable sol
1.25	4	1	1.00	stable sol

80% of etacac remaining in the final dry xerogel, according to the initial  $x$  and  $h$  values.

Polymerization of titanium butoxide. In the case of titanium butoxide, an exhaustive study was rendered impossible because of the high reactivity of this alkoxide that made it impossible to (1) to prepare sols and gels with etacac as the main complexant (the weak area reported for a precipitate in Table 1 contrasts with the usually relatively high area in the case of gels) and (2) to allow  $h$  to vary significantly once  $x$  was chosen. A gelification diagram (with acac) has, however, been reported in the literature in slightly different conditions than ours, which shows that both  $x$  and  $h$  play an important role, with sols always obtained at low  $h$  values.<sup>15</sup> Therefore, only selected experiments were performed and the results are presented in Tables 2 and 3. Again a  $D$  plateau is reached, extremely quickly in this case, and in all cases but one the first measurement after water addition reaches the  $D$  plateau. Values have been therefore gathered in Tables 2 and 3 according to the probe kind.

## Discussion

In the framework of the theoretical approach defined, it is clear that in the zirconium systems the  $D$  drop measured by chronoamperometry is directly related to the size of the polymers formed. Variations are large enough to provide information on both the evolution and the final state of the systems. It is noticeable in the framework of our theoretical approach that the influence of the electron transfer between small and big oligomers would be that the apparent diffusion coefficient value



gets closer to the mean value than it would in the case of a simple additive behavior. Especially in the case of a Gaussian distribution of the diffusion coefficient, the apparent value stays extremely close to the average value, when the  $\sigma$  value does not exceed 40% of the  $D_\mu$  value, due to the diffusion coupled electron exchange. We have also checked that integrating the curves from zero instead of 1 (reducing the monomer mass or diffusion coefficient to its lowest possible limit) almost does not change the curves displayed in Figures 3 and 4.

**Kinetic Behavior.** The very fast  $D$  decay on all curves proves that the polycondensation reactions begin within seconds as soon as water addition occurs; therefore confirming the high reactivity of the alkoxide even with complexant added. To explain such fast polymerization, it should be admitted that hydrolysis is almost instantaneous as soon as water is introduced in the system. It is somewhat surprising that the time to reach the  $D$  plateau, which is characteristic of the condensation kinetics of the system, appears more dependent on the plateau value than the ligand nature, suggesting that the condensation has comparable kinetics whatever the main ligand (probably related to mixing). Only in the case where acac (which is the best of the two complexants that we tried) is used, with a low hydrolysis ratio, is a time-dependent kinetics observable (Figure 5b). Although the hydrolysis ratio has a very weak influence on the final  $D$  plateau value, it may influence the rapidity at which this value is attained. Probably both less hydrolyzed species are formed and their condensation is slower, again especially in the case where acac is the main ligand. This idea is attested by the results in Figure 8, which show that the same  $D$  value is reached at clearly different rates due to the difference in the hydrolysis ratios. On the contrary, Figure 5a (case where etacac is the main ligand) does not show any appreciable difference concerning the time at which the plateau is reached, arguing thus for a relatively rapid hydrolysis of the etacac ligand.

**$D$  Plateau.** In all cases, we observed that a limit plateau was reached for  $D$ , which varies both with the system and the probe nature. In the case where salicylate is the anchor of the probe, there was no release of the probe. As explained before, ultramicroelectrode experiments did not show any noticeable depletion of the electroactive species concentration, and therefore the  $D$  drop experienced by the chronoamperometry is related to a slowing down of the diffusion of the grafted electroactive species. However, the interpretation of this value is not straightforward, although it should be related to the average mass of the oligomers when the condensation reaction has stopped. As often noticed before in different sol-gel systems, the gel time is not a relevant parameter because a plateau in the  $D$  value is usually reached before the gel time. This argues for the  $D$  plateau to be directly related to the diffusion of the grafted species because if restricted diffusion were to occur, then gelification and the first stages of aging would influence the plateau value. As we discussed before, there is only a slight deviation from the average diffusion coefficient provided that the distribution of masses was not too extended and thus the  $D$  plateau experienced by the Fc-sal probe reflects the average diffusion coefficient of inorganic oxopolymers onto which the ferrocenic species have been grafted. This assertion is supported by the results displayed Figure 7a, where clearly the plateau currents are inversely proportional to the complexation ratio. This is in accordance with literature results because it is known that the lowest is the complexation ratio and the highest is the size of the oligomers. From the diffusion coefficient determination, we can try to evaluate the average size of the oxopolymers formed, continuing to suppose that the

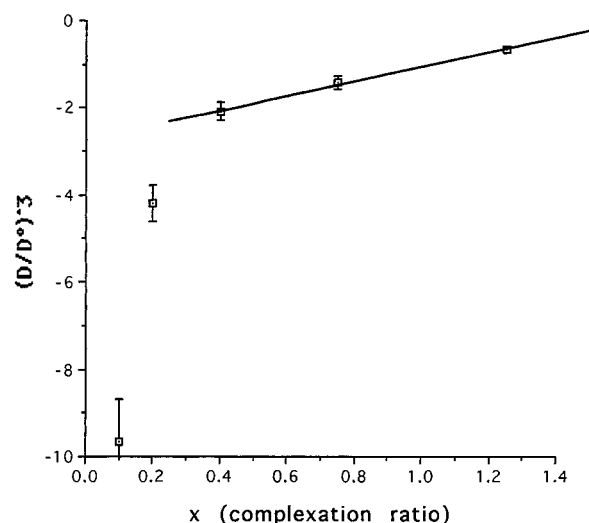


**Figure 9.** Plot of the  $(D/D^\circ)^3$  variation with the complexation ratio  $x$  (couple Fc-sal/etacac), deduced from the data in Figure 6.

$D/D^\circ$  values are proportional to the power 1/3 of the reduced mass  $m/m^\circ$ ,  $m^\circ$  being the monomer mass. Figure 9 shows that in the sols and slow gels, the dependence of  $(D/D^\circ)^3$  correlates with the complexation ratio. However, in the domain of the turbid gels and precipitates, the correlation stops and the linearity of the plot ceases. If, as expected, the  $(D/D^\circ)^3$  is really correlated to the reduced mass variation, it comes  $\ln(m/m^\circ) = kx$ . Then, the average mass of the final polymers would vary exponentially with the complexation rate, which is not unexpected in the case of an aggregating process and a second-order kinetics in each elementary step. Moreover, the BET surface area of the dried gels may be correlated with the average oligomer size, on the (very approximated) basis of sphere stacking; with most dried gels, the diameter of the spheres would be in the 50–100 Å range. This result is not in contradiction with the mass of the oxopolymers experienced by the electrochemical study, which falls between 10 and 1000 times the mass of the functionalized monomer according to the hydrolysis conditions.

In the case of titanium butoxide, the results in Table 2 show very clearly that when Fc-acac is the functionalized ligand, there is no variation at all in the diffusion coefficients, whatever the conditions chosen ( $x$  and/or  $h$  values, sols or gels). This result shows unambiguously that Fc-acac is not able to compete with acac, this contrasting with the more ambiguous situation met in the case of zirconium propoxide. The results in Table 3 show, on the contrary, that in the case of Fc-sal as the functionalized probe there is a strong variation encountered in the case of gelling systems (weak  $x$  and relatively high  $h$  values), whereas in the case of stable sols, there is almost no drop noticed, as a probable consequence of the formation of low molecular weight clusters. This situation shows again that Fc-sal is strongly bound to the polymerizing species and that with weak complexation ratios, a sharp drop is noticed as the consequence of the very fast formation of highly condensed species. This result is confirmed by the high specific area reported in Table 1 for such gels.

## Conclusion

The electrochemical approach where an electroactive species is bound to the metal center is an efficient technique to follow the aggregation process occurring during the polymerization of metal propoxides. Experiments of functionalized ligand bound

to zirconium species in the course of polymerization, showed that, as expected, the average measured diffusion coefficient reflects the mass of the oxopolymers formed when the electrochemical probe is bound with a strongly anchoring species like the salicylate function. We have shown that, especially in the case of the weakly complexing etacac as a ligand, the average mass of the polymers formed is experienced by the diffusion coefficient determined from the electrochemical measurements. In the case of titanium species, we have shown that the polymerization was extremely fast, and that complexation on titanium species was less efficient because the Fc-acac probe does not bind at all in the presence of free acac in the medium. The theoretical prediction for the response of electroactive species in the presence or without diffusion-coupled electron transfer has been solved out and shows that in the case of a Gaussian distribution, there is only a slight difference between the current from a real collection of species, and the current that would be recorded if all the species had the central mass. Therefore the average diffusion coefficient reflects with a reasonable accuracy the actual diffusion coefficient of the midpoint species, even when there is a noticeable dispersion of the molecular weights of the species.

**Supporting Information Available:** Figures of experimental data from an experiment using ultramicroelectrodes and of experimental diffusion coefficients vs time (2 pages). Ordering information is on any current masthead page.

## References and Notes

- (1) (a) Livage, J.; Henry, M.; Sanchez, C. *Prog. Solid State Phys.* **1988**, *18*, 259; (b) Sanchez C.; Ribot, F. *New J. Chem.* **1994**, *18*, 1007.
- (2) (a) Brinker, C. J.; Scherrer, G. *Sol-Gel Science, the Physics and Chemistry of Sol-gel Processing*; Academic: San-Diego, 1989; (b) Babonneau, F. *Mater. Res. Soc. Symp. Proc.* **1994**, *346*, 949.
- (3) (a) Audebert, P.; Griesmar, P.; Sanchez, C. *J. Mater. Chem.* **1991**, *1*, 699; (b) Audebert, P.; Griesmar, P.; Hapiot, P.; Sanchez, C. *J. Mater. Chem.* **1992**, *2*, 1293; (c) Cattey, H.; Audebert, P.; Hapiot, P.; Sanchez, C. *J. Mater. Chem.* **1997**, *7*, 1461.
- (4) (a) Sanchez, C.; Ribot, F.; Doeuff, S. In *Inorganic and Organic Polymers with Special Properties*, Nato ASI Series; Laine, R. M., Ed.; Kluwer: New York, 1992; Vol. 206, p 267; (b) Mehrotra, R. C.; Bohra, R.; Gaur, D. P. *Metal b-Diketonates and Allied Derivatives*; Academic: London, 1978; (c) Yoldas, B. E. *J. Mater. Sci.* **1986**, *21*, 1086.
- (5) (a) Kapoor, R. N.; Mehrotra, R. C. *J. Am. Chem. Soc.* **1960**, *82*, 3495; (b) Griesmar, P. Thesis, University of Paris 6, July 1992.
- (6) (a) Sanchez, C.; In, M. *J. Non-Cryst. Solids* **1992**, *1*, 147; (b) French patents nos. INPI 91 11634, 91 11635 (In, M.; Sanchez, C.; Daniel J. C.); (c) In, M. Thesis, University of Paris 6, June 1994.
- (7) Andrieux, C. P.; Hapiot, P.; Savéant, J.-M. *J. Electroanal. Chem.* **1984**, *49*, 172.
- (8) Garreau, D.; Savéant, J.-M. *J. Electroanal. Chem.* **1972**, *35*, 309.
- (9) Shoup, D.; Szabo, A. *J. Electroanal. Chem.* **1982**, *140*, 237.
- (10) Andrieux, C. P.; Savéant, J.-M. *J. Electroanal. Chem.* **1970**, *28*, 339.
- (11) (a) Miller, S. L.; Orleman, E. F. *J. Am. Chem. Soc.* **1953**, *75*, 2001; (b) Schwall, R. J.; Smith, D. E. *J. Electroanal. Chem.* **1978**, *94*, 227; (c) Andrieux, C. P.; Hapiot, P.; Savéant, J.-M. *J. Electroanal. Chem.* **1985**, *186*, 237; (d) Evans, D. H. *J. Electroanal. Chem.* **1989**, *258*, 451.
- (12) (a) Deksibar, J. C. *J. Non Cryst. Solids* **1986**, *87*, 343; (b) Deksibar, J. C. *J. Mat. Sci.* **1985**, *20*, 44; (c) Livage, J.; Sanchez, C. *J. Non Cryst. Solids* **1992**, *145*, 11; (d) Papet, P.; LeBars, N.; Baumard, J. F.; Lecomte, A.; Dager, A. *J. Mater. Sci.* **1989**, *24*, 3850.
- (13) Saxena, U. B.; Rai, A. K.; Mathur, V. K.; Mehrotra, R. C.; Bradford, D. *J. Chem. Soc., A* **1970**, 904.
- (14) (a) Amatore, C.; Azzabi, M.; Calas, P.; Jutand, A.; Lefrou, C.; Rollin, Y. *J. Electroanal. Chem.* **1990**, *288*, 45; (b) Denuault, G.; Mirkin, M. V.; Bard, A. J. *J. Electroanal. Chem.* **1991**, *308*, 27.
- (15) Bleuzen, A.; Barbox-Doeuff, S.; Flaud P.; Sanchez, C. *Mater. Res. Bull.* **1994**, *29*, 1223.